Supplementary Figure 1 | Venom peptide Ta2a from *T. africanum* is related to M-MYRTX-Tb1a (also known as bicarinalin) from venom of the ant *T. bicarinatum*. Alignment of the precursor sequence of Ta2a and M-MYRTX-Tb1a. Signal peptides and mature peptides are underlined in purple and black, respectively. Lysine/arginine and aspartate/glutamate residues are highlighted in blue and red, respectively.

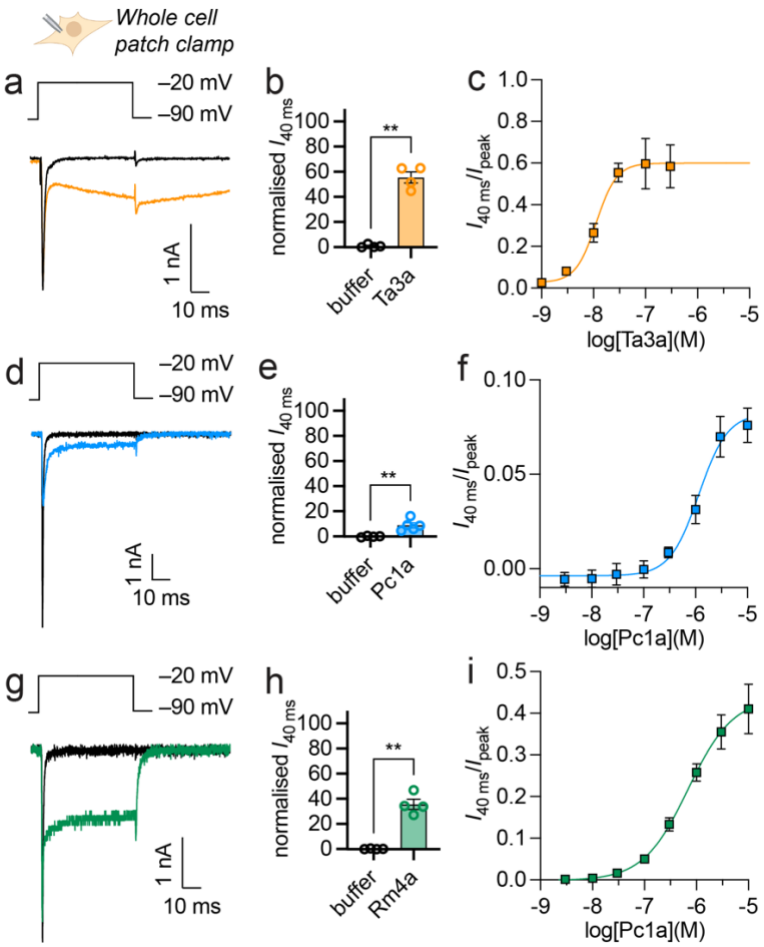

Supplementary Figure 2 | Ant venom peptides Ta3a, Pc1a and Rm4a modulate mouse Nav1.7. (a) Representative current response from a HEK293 cell expressing mNav1.7 to a step depolarization from –90 to –20 mV in the absence (black) and presence of Ta3a (30 nM, orange). Both traces shown are without leak subtraction. (b) Ta3a (30 nM) caused a sustained current of 55.4 ± 4.5 % of control peak; **, $P = 0.0013$; paired *t*-test, two-sided; $n = 4$ cells. (c) Concentration-response relationship for Ta3a modulation of mNav1.7 where response is sustained current ($I_{40\text{-ms}}$)/peak current (I_{max}) ($n = 4$ cells). (d) Representative current response from a HEK293 cell expressing mNav1.7 to a step depolarization from –90 to –20 mV in the absence (black) and presence of Pc1a (3 µM, blue). (e) Pc1a (3 µM) caused a sustained current of 8.8 ± 2.0 % of control peak; **, $P = 0.0085$; paired *t*-test, two-sided; $n = 5$ cells. (f) Concentration-response relationship for Pc1a modulation of mNav1.7 ($n = 5$ cells). (g) Representative current response from a HEK293 cell expressing mNav1.7 to a step depolarization from –90 to –20 mV in the absence (black) and presence of Rm4a (3 µM, green). (h) Rm4a (3 µM) causes a sustained current of 35.5 ± 4.1 % of control peak; **, $P = 0.0032$; paired *t*-test, two-sided; $n = 4$ cells. (i) Concentration-response relationship for Rm4a modulation of mNav1.7 ($n = 4$ cells). Data are expressed as mean ± SEM. Source data are provided as a Source Data file.

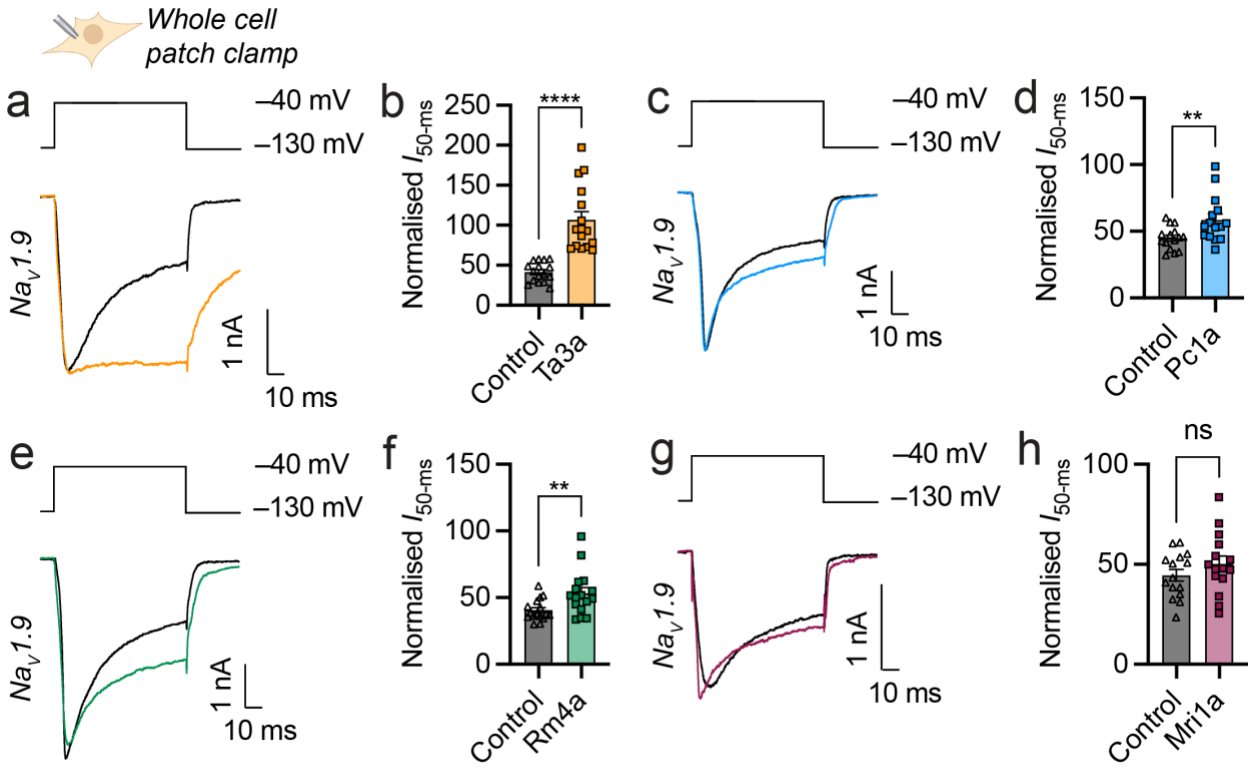

Supplementary Figure 3 | Ant venom peptides Ta3a, Pc1a and Rm4a modulate Nav1.9. (a) Representative current response from a HEK293 cell expressing hNaV1.9 to a step depolarization from –130 to –40 mV in the absence (black) and presence of Ta3a (1 µM, orange). (b) NaV1.9 sustained current (current amplitude at 50-ms) evoked by a step depolarization from –130 to –40 mV before (control) and after treatment with Ta3a (1 µM), expressed as % of control I_{peak}. ****, $P < 0.0001$ (unpaired *t*-test; two-sided; $n = 16$ cells). (c-d) Equivalent data for Pc1a (1 µM) ($n = 15$ cells). (e-f) Equivalent data for Rm4a (1 µM). **, $P = 0.0032$ (unpaired *t*-test; two-sided; $n = 16$ cells). (g-h) Equivalent data for Mri1a (1 µM). n.s., not significant (unpaired *t*-test; two-sided; $n = 16$ cells). Data are expressed as mean ± SEM. Source data are provided as a Source Data file.

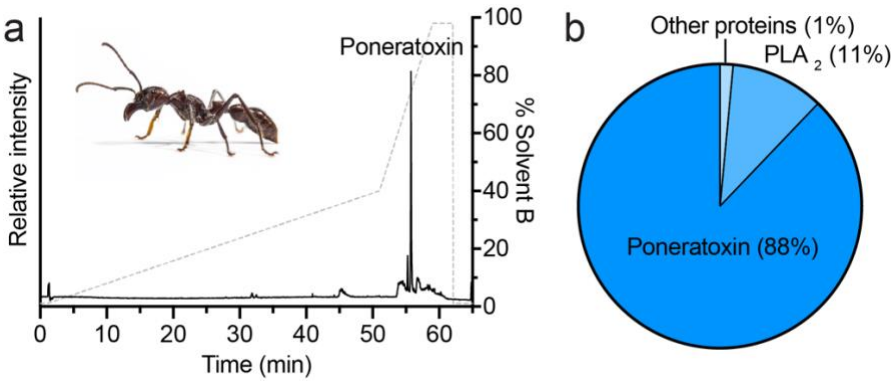

Supplementary Figure 4 | The venom of *P. clavata* is composed near-exclusively of the peptide poneratoxin. (**a**) Total ion chromatogram of *P. clavata* venom. The peak corresponding to poneratoxin is labelled. (**b**) Poneratoxin is the most highly expressed venom component-encoding transcript (defined as transcripts that encode peptides/proteins detected in the venom by LC-MS/MS) in the published venom gland transcriptome of *P. clavata*[1] where it constitutes 88% (52,149 of 59,364 transcripts per million) of venom component-encoding reads. PLA_2, phospholipase A_2.

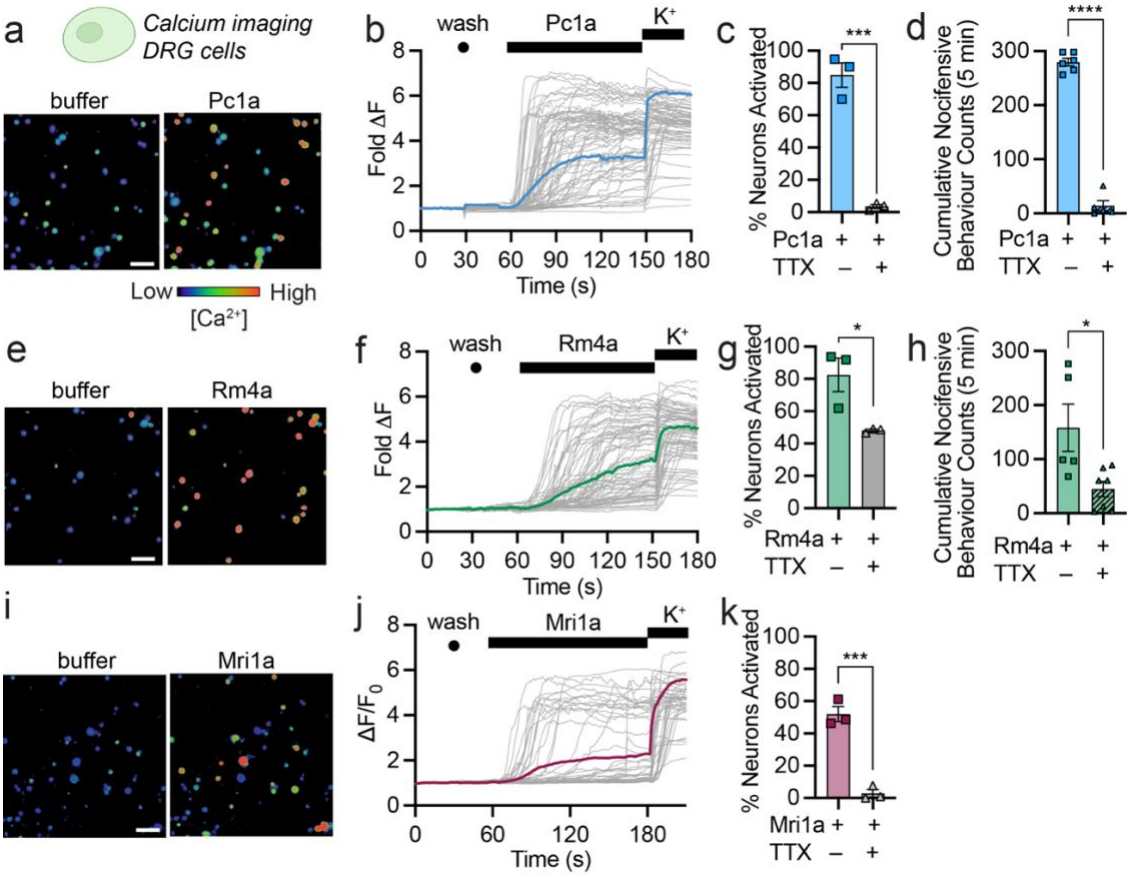

Supplementary Figure 5 | Ant venom peptide-induced activation of mouse DRG neurons and spontaneous nocifensive behaviours in mice are reduced by tetrodotoxin (TTX). (a) Representative (of 3 independent repeats) pseudocolour images illustrating $[Ca^{2+}]_i$ in DRG neurons before (buffer) and after application of Pc1a (500 nM); scale bar = 100 µm. (b) Time course of individual DRG neuron responses to Pc1a (of 3 independent repeats). Each trace represents an individual neuron. The blue trace represents the average response; K^+, 30 mM KCl (positive control). (c) Percentage of DRG neurons activated by Pc1a (500 nM) in the absence or presence of TTX (1 µM). ***, $P = 0.0004$ (unpaired *t*-test; two-sided; $n = 3$ independent experiments). (d) Pc1a (60 pmol)-induced spontaneous nocifensive behaviours with or without co-injection of 2 µM TTX. ****, $P < 0.0001$ (unpaired *t*-test; two-sided; $n = 6$ mice per group). (e) Representative (of 3 independent repeats) pseudocolour images illustrating $[Ca^{2+}]_i$ in DRG neurons before (buffer) and after application of Rm4a (500 nM). (f) Time course of individual DRG neuron responses to Rm4a (representative of 3 independent repeats). (g) Percentage of DRG neurons activated by Rm4a (500 nM) in the absence or presence of TTX (1 µM). ***, $P = 0.00297$ (unpaired *t*-test; two-sided; $n = 3$ independent experiments). (h) Cumulative spontaneous nocifensive behaviours in mice after intraplantar injection of saline or TTX (2 µM), 30 min after injection of Rm4a (60 pmol). *, $P = 0.0175$ (unpaired *t*-test; two-sided; $n = 5$ mice per group). (i) Representative (of 3 independent repeats) pseudocolour images illustrating $[Ca^{2+}]_i$ in DRG neurons before (buffer) and after application of Mri1a (1 µM). (j) Time course of individual DRG neuron responses to Mri1a (representative of 3 independent repeats). (k) Percentage of DRG neurons activated by Mri1a (1 µM) in the absence or presence of TTX (1 µM). ***, $P < 0.0007$ (unpaired *t*-test; two-sided; $n = 3$ independent experiments). Data are expressed as mean ± SEM. Source data are provided as a Source Data file.

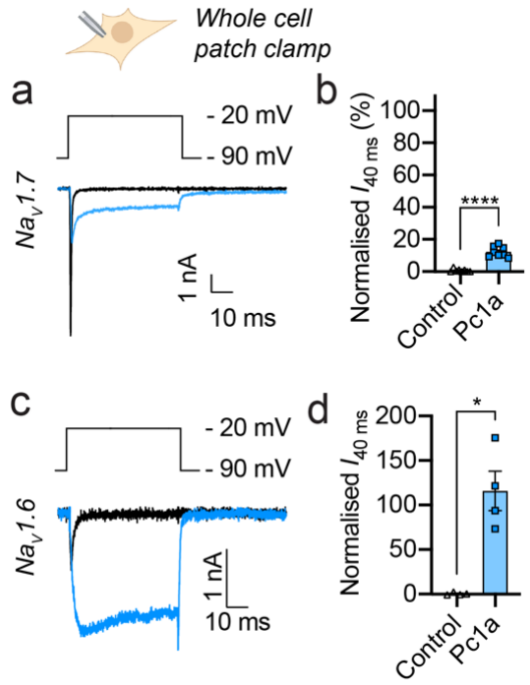

Supplementary Figure 6 | Poneratoxin (Pc1a) modulates hNaV1.7 and hNaV1.6. (a) Representative hNaV1.7 current response to a step depolarisation from –90 to –20 mV in the absence (black) and presence of 3 µM Pc1a (blue). (b) hNaV1.7 sustained current (current amplitude at 40-ms) evoked by a step depolarisation from –90 to –20 mV before (control) and after treatment with Pc1a (3 µM), expressed as % of control I_{peak} (n = 6 cells). (c) Representative hNaV1.6 current response to a step depolarisation from –90 to –20 mV in the absence (black) and presence of 3 µM Pc1a (blue). (d) hNaV1.6 sustained current (current amplitude at 40-ms) evoked by a step depolarisation from –90 to –20 mV before (control) and after treatment with Pc1a (3 µM), expressed as % of control I_{peak} (n = 4 cells). Data are expressed as mean ± SEM; ****, $P < 0.0001$; *, $P < 0.05$ (unpaired t-test; two-sided). Source data are provided as a Source Data file.

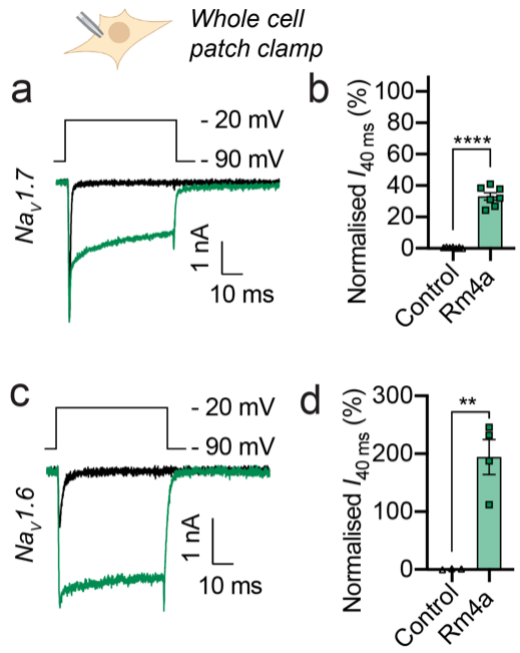

Supplementary Figure 7 | Rm4a modulates hNaV1.7 and hNaV1.6. (a) Representative hNaV1.7 current response to a step depolarisation from –90 to –20 mV in the absence (black) and presence of 3 µM Rm4a (green). (b) hNaV1.7 sustained current (current amplitude at 40-ms) evoked by a step depolarisation from –90 to –20 mV before (control) and after treatment with Rm4a (3 µM), expressed as % of control I_{peak} (n = 7 cells). (c) Representative hNaV1.6 current response to a step depolarisation from –90 to –20 mV in the absence (black) and presence of 3 µM Rm4a (green). (d) hNaV1.6 sustained current (current amplitude at 40-ms) evoked by a step depolarisation from –90 to –20 mV before (control) and after treatment with Rm4a (3 µM), expressed as % of control I_{peak} (n = 4 cells). Data are expressed as mean ± SEM; ****, P < 0.0001; **, P < 0.01 (unpaired t-test; two-sided). Source data are provided as a Source Data file.

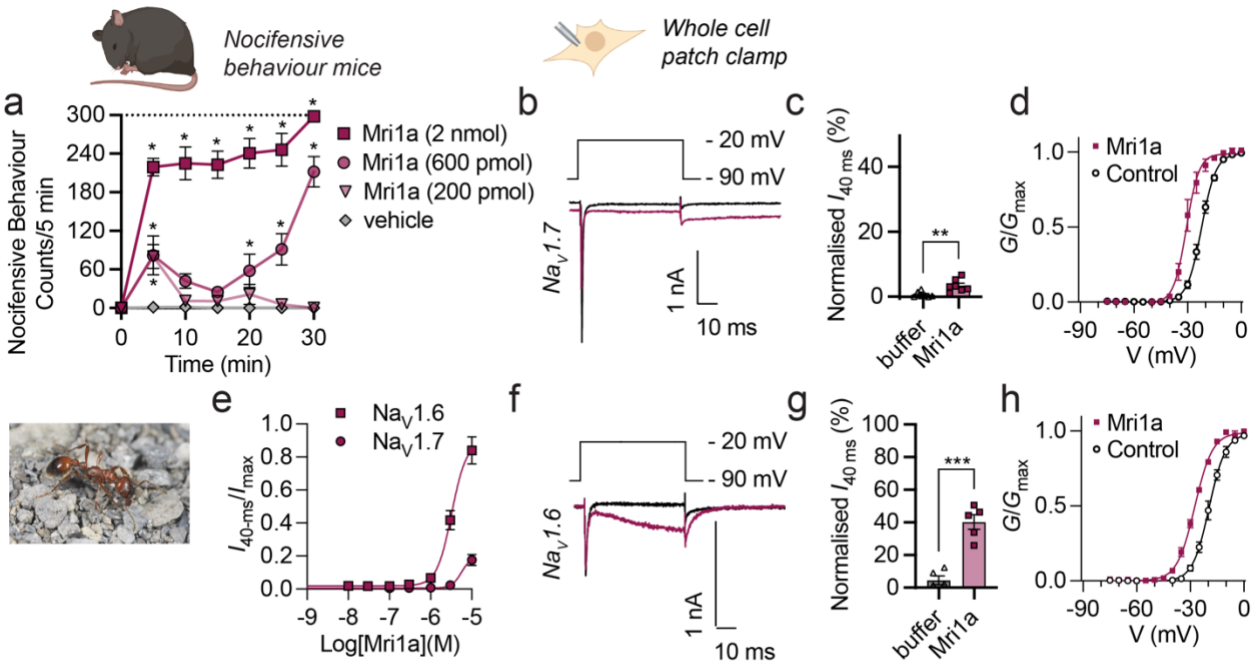

Supplementary Figure 8 | Activity of Mri1a from the venom of *M. rubida*. (a) Spontaneous nocifensive behaviours in mice following shallow intraplantar injection of Mri1a (n = 3 mice per group). *, $P < 0.05$ (two-way ANOVA with Holm-Šídák's multiple-comparisons to negative control). Inset: *M. rubida* worker (~7 mm in length). Photo credit: Thibaud Monnin. (b) Representative hNav1.7 current response (without leak subtraction) to a step depolarisation from –90 to –20 mV in the absence (black) and presence of 3 µM Mri1a (maroon). (c) Nav1.7 sustained current (current amplitude at 40-ms) evoked by a step depolarisation from –90 to –20 mV before (control) and after treatment with Mri1a (3 µM), expressed as % of control I_{peak} **, P = 0.0061; unpaired t-test, two-sided; n = 7 cells. (d) Nav1.7 G-V curve, before (white) and after addition of 3 µM Mri1a (maroon) (n = 5 cells). (e) Concentration-response relationship for Mri1a modulation of hNav1.6 (n = 5 cells) and hNav1.7 (n = 7 cells), where response was [(sustained current ($I_{40\text{-ms}}$) after Mri1a treatment)/(peak current (I_{peak}) before treatment (control)]. (f) Representative hNav1.6 current response (without leak subtraction) to a step depolarisation from –90 to –20 mV in the absence (black) and presence of 3 µM Mri1a (maroon). (g) Nav1.6 sustained current (current amplitude at 40-ms) evoked by a step depolarisation from –90 to –20 mV before (control) and after treatment with Mri1a (3 µM), expressed as % of control I_{peak}. ***, P = 0.0007; unpaired t-test, two-sided; n = 5 cells. (h) Nav1.6 G-V curve, before (white) and after addition of 3 µM Mri1a (maroon) (n = 3 cells). Data are expressed as mean ± SEM. Source data are provided as a Source Data file.

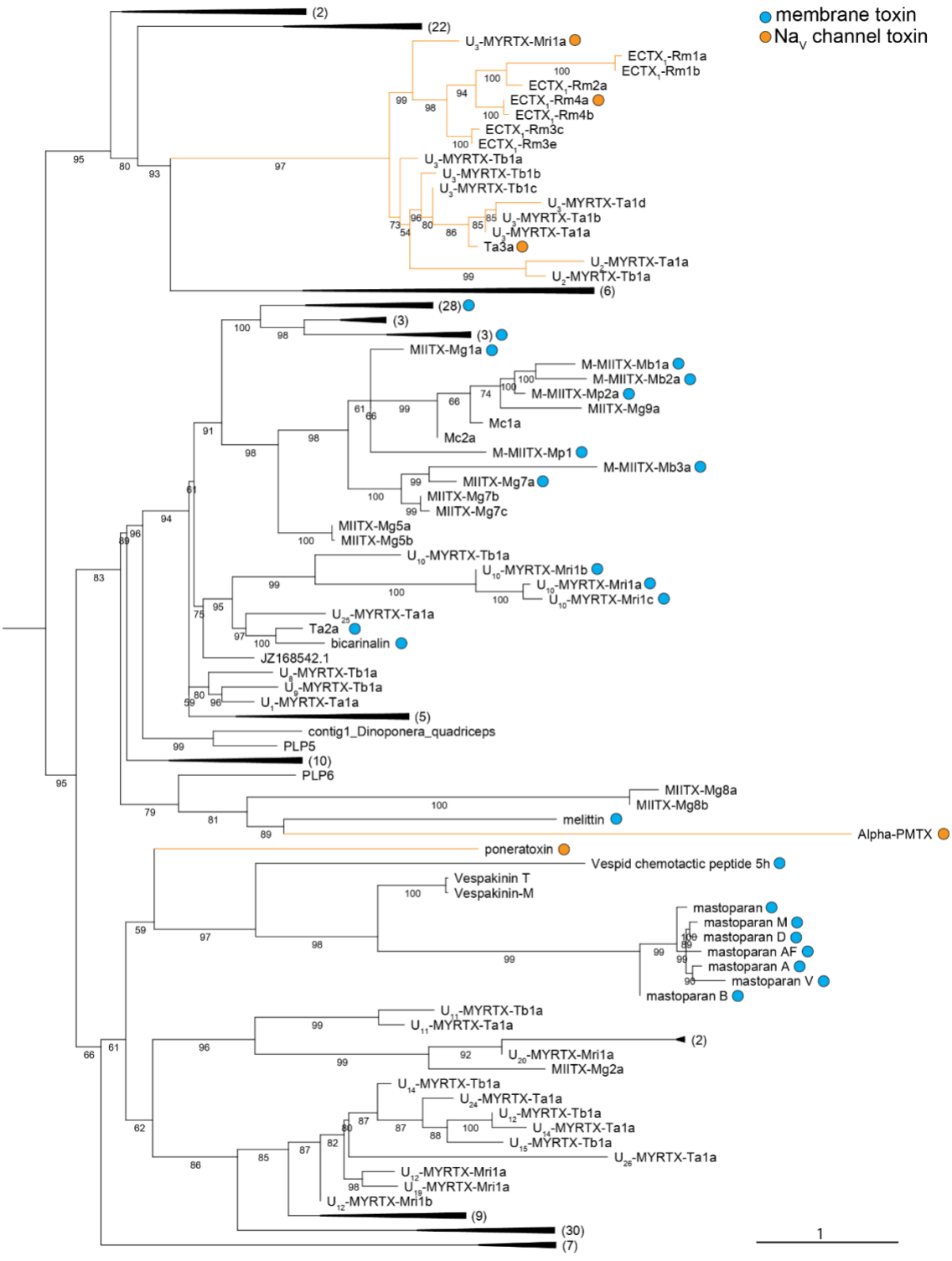

Supplementary Figure 9 | Phylogenetic reconstruction of the aculeatoxins. A maximum likelihood tree estimated using PhyML from an alignment of aculeatoxin precursor sequences. Branches representing hymenopteran venom Nav channel toxins are coloured orange. Bootstrap values are indicated under each node.

Supplementary Table 1. Potency (μM) of ant venom Na_V channel toxins at Na_V channel subtypes.

μM	Primary structure	$hNa_V1.6$	$hNa_V1.7$	$mNa_V1.7$	$hNa_V1.8$
Ta3a	LAPIFALLLLSGLFSLPALQHYIEKNYIN*	0.025 ± 0.002	0.030 ± 0.009	0.018 ± 0.005	0.33 ± 0.06
Pc1a	FLPLLILGSLLMTPPVIQAIHDAQR*	0.097 ± 0.010	2.3 ± 0.4	1.8 ± 0.2	>10
Rm4a	FPPLLLLAGLFSLPALQHYIETKWIN*	0.20 ± 0.02	1.9 ± 0.4	1.2 ± 0.2	8.4 ± 1.0
Mri1a	GLPLLALLMTLPFIQHAITN*	3.3 ± 0.4	>10	N.D.	N.D.

*, C-terminal amidation; N.D., not determined.

Supplementary References:

1 Aili, S. R. *et al.* An Integrated Proteomic and Transcriptomic Analysis Reveals the Venom Complexity of the Bullet Ant *Paraponera clavata*. *Toxins* **12**, (2020).